Li et al. *Zool. Res.* 2024, 45(5): 1048−1060
https://doi.org/10.24272/j.issn.2095-8137.2023.373
https://cstr.cn/32248.14.zr.2024.373

ZR | Zoological Research

Article Open Access

Cadherin-18 loss in prospermatogonia and spermatogonial stem cells enhances cell adhesion through a compensatory mechanism

Xiao-Xiao Li[1,2,#], Dan-Chen Zhang[1,2,#], Yan Wang[4,#], Jian Wen[1,2], Xing-Ju Wang[1,2], Yu-Lu Cao[1,2], Ru Jiang[1], Jia-Rui Li[1], Yi-Nuo Li[1], He-He Liu[1], Wen-Hai Xie[3], Zheng-Feng Xu[4,*], Ping Hu[4,*], Kang Zou[1,2,*]

[1] *Germline Stem Cells and Microenvironment Lab*, *College of Animal Science and Technology*, *Nanjing Agricultural University*, *Nanjing*, *Jiangsu* 210095, *China*

[2] *Stem Cell Research and Translation Center*, *Nanjing Agricultural University*, *Nanjing*, *Jiangsu* 210095, *China*

[3] *School of Life Sciences and Medicine*, *Shandong University of Technology*, *Zibo*, *Shandong* 255000, *China*

[4] *Department of Prenatal Diagnosis*, *Women's Hospital of Nanjing Medical University*, *Nanjing Maternity and Child Health Care Hospital*, *Nanjing*, *Jiangsu* 210004, *China*

ABSTRACT

Extracellular membrane proteins are crucial for mediating cell attachment, recognition, and signal transduction in the testicular microenvironment, particularly germline stem cells. Cadherin 18 (CDH18), a type II classical cadherin, is primarily expressed in the nervous and reproductive systems. Here, we investigated the expression of CDH18 in neonatal porcine prospermatogonia (ProSGs) and murine spermatogonial stem cells (SSCs). Disruption of CDH18 expression did not adversely affect cell morphology, proliferation, self-renewal, or differentiation in cultured porcine ProSGs, but enhanced cell adhesion and prolonged cell maintenance. Transcriptomic analysis indicated that the down-regulation of *CDH18* in ProSGs significantly up-regulated genes and signaling pathways associated with cell adhesion. To further elucidate the function of CDH18 in germ cells, *Cdh18* knockout mice were generated, which exhibited normal testicular morphology, histology, and spermatogenesis. Transcriptomic analysis showed increased expression of genes associated with adhesion, consistent with the observations in porcine ProSGs. The interaction of CDH18 with β-catenin and JAK2 in both porcine ProSGs and murine SSCs suggested an inhibitory effect on the canonical Wnt and JAK-STAT signaling pathways during CDH18 deficiency. Collectively, these findings highlight the crucial role of CDH18 in regulating cell adhesion in porcine ProSGs and mouse SSCs. Understanding this regulatory mechanism provides significant insights into the testicular niche.

Keywords: Extracellular signal; Fertility; Quiescency; Wnt signaling pathway

INTRODUCTION

Prospermatogonia (ProSGs) serve as the precursors to spermatogonial stem cells (SSCs) in the immature testis. During embryonic development, primordial germ cells migrate to the genital ridge, where they form gonadal cells, also known as gonadotropic cells (Clermont & Perey, 1957; Yamada et al., 2016). After birth, these gonadal cells undergo mitosis and migrate from the center to the basement membrane of the spermatogenic tubules, forming the SSC pool that sustains spermatogenesis throughout life (McGuinness & Orth, 1992). The balance between SSC self-renewal and differentiation is critical for maintaining spermatogenesis (Caires et al., 2010; Dadoune, 2007; De Rooij & Russell, 2000; Kubota & Brinster, 2006), a process regulated by the testicular microenvironment (Kanatsu-Shinohara et al., 2005). In mice, ProSGs begin migrating to the niche on day 2 post-birth and complete this by day 5 to form SSCs, while in pigs, spermatogonia emerge around two months of age and finish migrating by 120 days (Goel et al., 2007).

In mice, both ProSGs derived from 2–3-day-old testes and SSCs derived from 5–10-day-old testes exhibit similar characteristics *in vitro*, including maintenance, expression

This is an open-access article distributed under the terms of the Creative Commons Attribution Non-Commercial License (http://creativecommons.org/licenses/by-nc/4.0/), which permits unrestricted non-commercial use, distribution, and reproduction in any medium, provided the original work is properly cited.

Copyright ©2024 Editorial Office of Zoological Research, Kunming Institute of Zoology, Chinese Academy of Sciences

Received: 01 April 2024; Accepted: 12 April 2024; Online: 13 April 2024

Foundation items: This study was supported by the Jiangsu Seed Industry Revitalization Project (JBGS[2021]024), Fundamental Research Funds for the Central Universities (KYT2023002), Jiangsu Province Capability Improvement Project through Science, Technology, and Education Jiangsu Provincial Medical Key Discipline (ZDXK202211), and Shandong Province Natural Science Foundation (ZR2020MC074)

[#]Authors contributed equally to this work

*Corresponding authors, E-mail: zhengfengxu@njmu.edu.cn; njfybjyhuping@163.com; kangzou@njau.edu.cn

profiles, and ability to restore spermatogenesis after transplantation. Transplantation of SSCs or ProSGs into the normal testicular microenvironment can successfully restore spermatogenesis in the recipient (Brinster, 2002; Brinster & Zimmermann, 1994; Orwig et al., 2002), making them ideal models for breeding, clinical applications, and gene therapy. Consequently, SSCs and ProSGs are considered equally suitable for genetic manipulation and research. Currently, however, culturing porcine SSCs *in vitro*, especially from adult testes, remains a challenge (Sun et al., 2019). Testes from 7–10-day-old piglets, commonly available from castration, provide a more accessible source of ProSGs, which sometimes exhibit better cell vitality than SSCs. However, the limited number of ProSGs in mammalian testes poses a significant challenge. Although the *in vitro* culture techniques for rodent SSCs are well established, they often fall short when applied to large mammals such as pigs, likely due to differences in essential factors and feeder requirements (Aponte et al., 2008; Sahare et al., 2016; Zheng et al., 2013). Studies have shown that porcine SSCs can be cultured *in vitro* for up to two months under standard conditions (Zhang et al., 2017). While various growth factors, additives, and culture conditions have been validated for ProSGs (Zheng et al., 2013), the *in vitro* culture system still requires improvement, especially for stable maintenance *in vitro*, which is crucial for applications such as gene editing, transplantation, and differentiation induction. A feeder layer is vital for the *in vitro* culture and attachment of germline stem cells, as detached cells tend to differentiate or undergo apoptosis (Fujihara et al., 2011; Lee et al., 2013, 2016; Song et al., 2022; Zhang et al., 2017, 2018; Zou et al., 2019). According to our previous experience, ProSGs have a relatively low affinity for Sertoli cell or mouse embryonic fibroblast (MEF) feeders compared to rodent SSCs. Thus, enhancing feeder affinity may benefit the *in vitro* culture of ProSGs.

Cadherins (CDH), a class of calcium-dependent cell adhesion molecules, are glycated transmembrane proteins essential for various morphogenetic events (Foty & Steinberg, 2005; Hogan et al., 2004; Johnson et al., 2004; Luo et al., 2004; Maeda et al., 2005; Reintsch et al., 2005). Classical cadherins are categorized into type I and type II based on their amino acid arrangement (Suzuki et al., 1991). Type I cadherins include E-cadherins (epithelial), N-cadherins (nerve), P-cadherins (placenta), and R-cadherins (retinal), which share the basic structure of the cadherin family. Type II cadherins, which differ from type I cadherins in specific amino acid sequences (Suzuki et al., 1991; Tanihara et al., 1994a, 1994b), include human cadherin-5, -6, -8, -11, and -12, as well as other type II cadherins found in mice, rats, chickens, and *Xenopus* (Espeseth et al., 1995; Kimura et al., 1995; Nakagawa & Takeichi, 1995). Cadherins are genetically conserved across species, playing important functional roles in cell adhesion, signal transduction, and cell fate regulation (Brigidi & Bamji, 2011; Halbleib & Nelson, 2006; Hirano & Takeichi, 2012; Redies, 2000). The *CDH18* gene encodes type II classical cadherins, which mediate calcium-dependent intercellular adhesion. CDH18 also plays a key role in biological processes such as central nervous system development and heart development (Chen et al., 2017; Junghof et al., 2022). Although research suggests that *CDH18* is also expressed in germline cells, its exact role remains unclear.

In the present study, we explored the expression of *CDH18* in ProSGs and its effects on cell fate and differentially expressed genes (DEGs). Morphological and transcriptomic analyses revealed that CDH18 plays a crucial role in ProSG adhesion. These findings provide valuable insights for improving the *in vitro* culture of ProSGs.

MATERIALS AND METHODS

Animals

Testicular samples were obtained from 7-day-old crossbred piglets (Duroc×Large White Yorkshire) after castration. The samples were transported to the laboratory within 2 h in D-Hanks buffer containing dual antibodies. The *Cdh18* knockout mice were generated by GemPharmatech. In brief, female C57BL/6J mice, treated with pregnant mare serum gonadotropin and human chorionic gonadotropin, were mated with male C57BL/6J mice, while non-hormone-injected female C57BL/6 mice were paired with vasectomized males to induce pseudo-pregnancy. Superovulated donor females were euthanized, and their fertilized oocytes were harvested. Cas/gRNA constructs, validated *in vitro*, were microinjected into the pronuclei of the fertilized oocytes from the C57BL/6Gpt background. The pseudo-pregnant females were then anesthetized, and the microinjected oocytes were transplanted into their oviducts. Successful implantation resulted in the birth of F0 generation mice after three weeks. Genomic DNA from 5–7-day-old F0 mice was extracted for PCR and sequencing to confirm genotypes. Upon reaching sexual maturity, the F0 mice were mated with wild-type C57BL/6J mice to obtain stable F1 heterozygous offspring, which were screened using PCR to identify mice heterozygous for the *Cdh18*-KO genotype.

All animal experiments were performed in accordance with the Regulations on the Management of Experimental Animals of Nanjing Agricultural University and were approved by the Ethics Committee of Nanjing Agricultural University and Nanjing Medical University.

Spermatogonial stem cell isolation, purification, and culture

SSCs were isolated using two-step enzymatic digestion (Wang et al., 2023). Initially, the tunica albuginea was removed from the surface of the testes of 7-day-old piglets. The testicular tissue was minced and digested with 1 mg/mL type IV collagenase for 30 min at 37°C, with pipetting every 10 min. Red blood cells were lysed at 4°C, with the resulting precipitate collected by centrifugation at 300 ×*g* for 5 min and washed with D-hanks buffer. The cells were then digested with 0.05% trypsin for 5 min at 37°C, after which digestion was terminated by the addition of 10% fetal bovine serum (FBS). The dispersed testicular cells were then filtered through a 70 μm cell sieve to obtain a single-cell suspension. The cells were subjected to differential adhesion in Dulbecco's Modified Eagle Medium/Nutrient Mixture F12 (DMEM/F12) containing 5% FBS, 1×double antibody, 1×GlutaMAX, 50 μmol/L β-mercaptoethanol, and 1×non-essential amino acids (NEAA) at intervals of 15 min, 30 min, 2–3 h, and overnight.

The following day, the cells were plated onto Sertoli cells pre-treated with mitomycin C for 3 h. The cells were then cultured at 35°C in DMEM/F12 supplemented with 100 IU/mL penicillin, 100 mg/mL streptomycin, 1×L-glutamine, 1×b27, 1×vitamin, 1×NEAA, 50 μmol/L β-mercaptoethanol, 1% bovine serum, 10% knockout serum replacement (KSR), 10 ng/mL

glial cell line-derived neurotrophic factor (GDNF), 10 ng/mL basic fibroblast growth factor (bFGF), and 20 ng/mL GFRα1. The cells were passaged for 5–6 days.

Reverse transcription polymerase chain reaction (RT-PCR)

Total RNA was extracted using TRNzol reagent (Tiangen, DP405, China) and cDNA was obtained by reverse transcription using a HiScript III All-in-one RT SuperMix Perfect for RT-PCR (Vazyme, R333-01, China) according to the manufacturer's instructions. PCR was performed using premixed 2×PCR mix (Vazyme, P213-03, China). Primer information is provided in Supplementary Table S1, Values were normalized to *GAPDH* expression.

Immunohistochemistry and immunofluorescence

Immunohistochemical and immunofluorescence analyses were conducted following established protocols (Wang et al., 2019). For immunohistochemistry, testicular samples were first fixed in neutral formalin, dehydrated, and embedded in paraffin. The tissues were then sectioned, deparaffinized, rehydrated with serial ethanol, and subjected to antigen repair using microwave heating. After blocking with 5% goat serum, the sections were incubated with primary antibodies and visualized using streptavidin-horseradish peroxidase (HRP) (Jackson Laboratory, USA) and a DAB kit (Vector, sk4100, USA). For immunofluorescence, ProSGs were seeded onto feeder layers or cell culture plates pre-coated with poly-L-lysine. After cell adhesion, the medium was removed, and the cells were washed once with phosphate-buffered saline (PBS). The cells were then fixed with pre-cooled Carnot fixator (methanol: glacial acetic acid=3:1) for 20 min at −20°C. Following fixation, the cells were washed 2–3 times with PBS, blocked with 10% goat serum for 30 min at 37°C, and incubated with primary antibodies overnight at 4°C. The next day, the cells were incubated with the corresponding secondary antibodies for 1 h at 37°C. After incubation, the cells were washed 2–3 times with PBS, stained with Hoechst 33342 at 37°C, and visualized using an Olympus inverted fluorescence microscope (Japan). The antibodies used in this study are listed in Supplementary Table S2.

Small interfering RNA (siRNA) transfection

The siRNAs were synthesized by GenePharma and transfected into ProSGs using Lipofectamine 3000 (Thermo Fisher, L3000-001, USA) according to the manufacturer's instructions. To verify siRNA knockdown efficiency, cells were harvested 72 h after transfection, RNA was isolated using TRNzol reagent, and gene expression levels were determined by RT-PCR. The siRNA sequences used in this experiment included CDH18 siRNA sense GGUUCUCGAUAGAGAA GAAAC and antisense UUCUUCUCUAUCGAGAACCUU.

Co-immunoprecipitation and western blotting

Testicular tissue was lysed with RIPA buffer containing a protease inhibitor mixture. After centrifugation at 16 000 ×*g* for 15 min, a portion of the supernatant was reserved as input, while the remainder was divided into four aliquots. Each aliquot was incubated overnight at 4°C with the corresponding antibody according to the manufacturer's instructions. The next day, agarose beads were washed 4–5 times and added to the protein lysates, followed by incubation at 4°C for 4 h. After centrifugation at 2000 ×*g* for 1 min, the supernatant was discarded, and the agarose beads were washed 4–5 times before heat elution. The proteins were then separated using 8% sodium dodecyl-sulfate polyacrylamide gel electrophoresis (SDS-PAGE) and blotted on a nylon membrane. The membranes were then blocked with 5% non-fat powdered milk in Tris-buffered saline with Tween 20 (TBST) and incubated with primary antibodies at 4°C overnight. After incubation, the membranes were washed with TBST three times and incubated with secondary antibodies at room temperature for 1 h (see antibodies information in Supplementary Table S2). The labeled proteins were visualized by enhanced chemiluminescence.

RNA-sequencing (RNA-seq)

At 72 h after CDH18 siRNA transfection, cells were harvested, and total RNA was extracted using TRNzol reagent. Sequencing libraries were constructed by Allwegene and sequenced following the manufacturer's protocols. Paired-end RNA-seq data consisted of 150 bp read lengths for each sample, with three biological replicates per group. FastQC (v.0.11.9) was used for quality control, Trim-Galore (v.0.6.10) was used for trimming and removing adapters, and HISAT2 (v.2.1.0) was used to align trimmed reads. The pig data were aligned to the *Sus scrofa* reference genome (ss11) and the mouse data were aligned to the *Mus musculus* reference genome (mm39). FeatureCounts (v.2.0.3) was used to quantitatively calculate the number of reads, with expression levels represented by Transcripts Per Kilobase per Million mapped reads (TPM). Differential expression analysis was conducted using DESeq2 (v.1.38.3), and DEGs were defined based on the $|\log_2\text{Fold-Change}|>0.5$ and *P*-adjusted>0.05 thresholds. Gene Ontology (GO) and Kyoto Encyclopedia of Genes and Genomes (KEGG) analyses were performed using the KOBAS database (http://kobas.cbi.pku.edu.cn/). Gene Set Enrichment Analysis (GSEA) was conducted using the clusterProfiler package (v.4.6.1). Results were visualized using the ggplot2 (v.3.4.1) package.

Statistical analysis

SSC counting was conducted following previous research (Song et al., 2022). ImageJ software (USA) was used for transcript expression analysis. The mRNA levels were normalized against *GAPDH* expression levels. All statistical analyses were conducted using GraphPad Prism v.8.01 (USA). Differences between groups were assessed using an unpaired *t*-test, with significant differences defined as *Q*-value<0.05.

RESULTS

Isolation and identification of porcine ProSGs

Porcine ProSGs express certain molecular markers, including protein gene product 9.5 (PGP9.5, also known as UCHL1) (Luo et al., 2006), promyelocytic leukemia zinc finger (PLZF), DEAD-box protein 4 (DDX4) (Gallardo et al., 2007; Niedenberger & Geyer, 2018), and glial cell-derived neurotrophic factor receptor alpha 1 (GFR α 1) (Lee et al., 2013). To determine the expression of DDX4 and PGP9.5 in ProSGs, testes from 7-day-old piglets were harvested and subjected to immunohistochemical analysis. $DDX4^+/PGP9.5^+$ cells were localized on the luminal basement membrane of seminiferous tubules and could be distinguished from surrounding somatic cells based on cell morphology (Figure 1A). Furthermore, Sertoli and germ cells were isolated and purified from the testes of 7-day-old piglets. Following differential attachment, ProSGs were enriched, purified, and

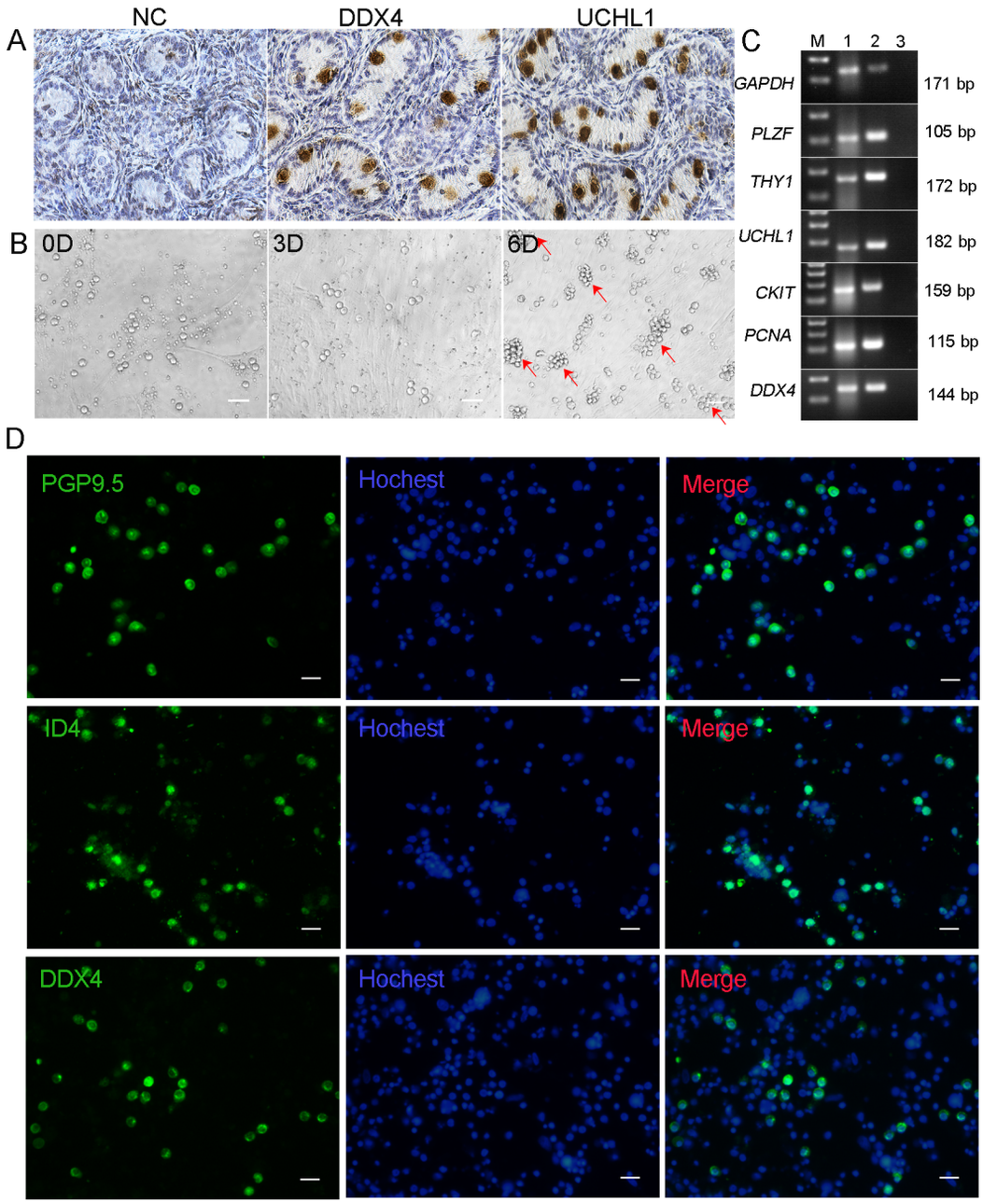

Figure 1 Characterization of porcine prospermatogonia isolated from piglets

A: Immunohistochemical staining of DDX4/UCHL1 in testes of 7-day-old piglets. B: Morphology of ProSGs cultured on Sertoli cells for different days (red arrows indicate grape-like colonies of ProSGs). C: Expression levels of ProSG markers *PLZF*, *THY1*, *UCHL1*, *c-KIT*, *PCNA*, and *DDX4* detected using RT-PCR. M, 1, 2, and 3 represent marker, testis, SSCs, and H_2O, respectively. D: Immunofluorescence staining for DDX4, ID4, and UCHL1 expression in ProSGs. Scale bar: 20 μm.

identified using immunofluorescence staining against UCHL1 (81.2%±1.78%) and PLZF (73.09%±1.56%) (Supplementary Figure S1A–H). Sertoli cells were purified using hypotonic treatment (Supplementary Figure S1I–L) and inactivated using mitomycin C. Purified ProSGs were seeded onto mitosis-inactive Sertoli cells to establish an *in vitro* co-culture system (Supplementary Figure S1M–P) (Zhang et al., 2020). During *in vitro* culture, newly isolated cells appeared round and transparent. After 2–3 days, cell clusters began to form. At day 5, ProSGs exhibited typical grape-like colonies with distinct cell boundaries, necessitating subculture at 5–6 days (Figure 1B). After four passages, the expression of ProSG markers *UCHL1*, *DDX4*, *PLZF*, *THY1*, *c-Kit*, and proliferation marker *PCNA* was assessed at the mRNA level using RT-PCR (Figure 1C). Additionally, the protein expression levels of UCHL1, inhibitor of differentiation 4 (ID4), and DDX4 were determined by immunofluorescence (Figure 1D), which indicated that ProSGs were stably maintained under these culture conditions.

Disturbance of *CDH18* using siRNA enhanced cell adhesion

To explore the function of CDH18 in ProSGs, ProSGs were transfected with scrambled siRNA or CDH18 siRNA. The efficiency of *CDH18* knockdown was confirmed at 72 h post-transfection, showing a 60%–70% decrease in *CDH18* expression (Figure 2A, B). During the latent and log phases of cell culture, no significant differences were observed in cell

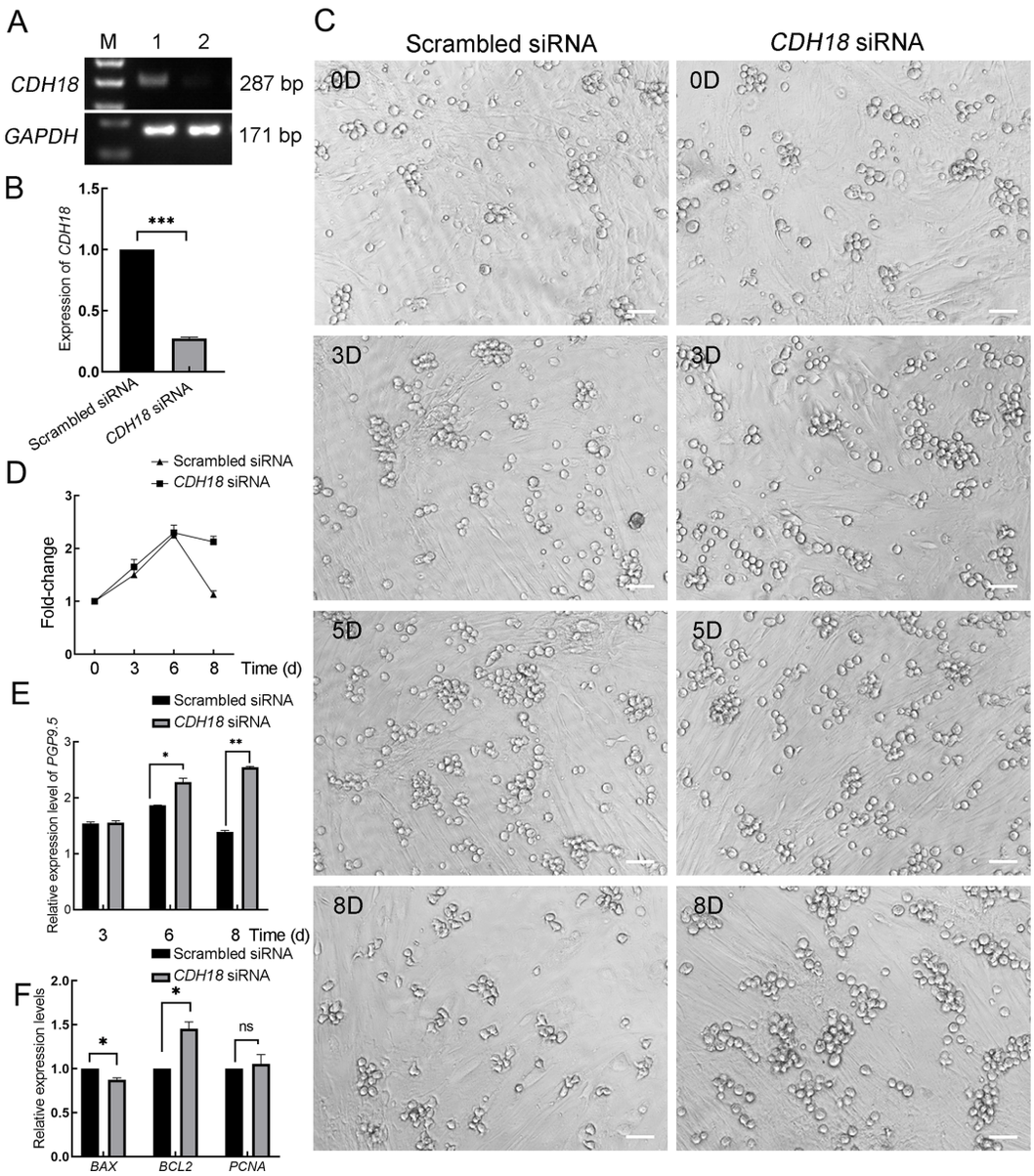

Figure 2 Consequences of *CDH18* knockdown in ProSGs

A: RT-PCR validation of *CDH18* suppression by specific siRNAs in ProSGs. B: Quantitative analysis of *CDH18* mRNA levels post-siRNA interference. C: Morphological alterations in ProSGs upon *CDH18* knockdown. D: Proliferative response measured by cell count following *CDH18* knockdown. E: Changes in expression of ProSG marker *PGP9.5* following *CDH18* knockdown. F: Changes in expression of *BAX*, *BCL2*, and *PCNA* following *CDH18* knockdown. Data are mean±standard deviation (SD), *: $P<0.05$; **: $P<0.01$; ***: $P<0.001$, ns: Not significant. Scale bar: 20 μm.

morphology, number, or proliferation between the experimental and control groups, with both maintaining a round and transparent state. However, as culture time increased, particularly over the passage time (5–6 days, entering the stationary and decline phases), some ProSGs in the control group detached from the feeder layer and floated in the culture medium. In contrast, the *CDH18* knockdown group showed no significant changes. By day 8, the number of floating and dead cells in the control group increased markedly, with a sharp decline in the remaining ProSGs on the feeder layer, while the interference group showed no significant change (Figure 2C, D). Consistently, the expression level of the ProSG marker *PGP9.5* began to decrease on day 6 in the scrambled siRNA-treated ProSGs and was significantly lower than that in the CDH18 siRNA-treated ProSGs by day 8 (Figure 2E). This confirmed that the number of ProSGs in the control group declined markedly from day 6, whereas ProSG numbers remained stable in the CDH18 siRNA-treated group even after 8 days of culture. Additionally, fresh ProSGs treated with scrambled or CDH18 siRNA for 6 days were harvested, and the expression levels of apoptotic marker *BAX*, anti-apoptotic marker *BCL2*, and proliferation marker *PCNA* were determined. The decreased expression of *BAX* and increased expression of *BCL2* in *CDH18* siRNA-treated ProSGs indicated that loss of *CDH18* inhibited apoptosis (Figure 2F). There was no significant difference in the proliferation ratio between the two groups (Figure 2F). These findings suggest that CDH18 may be associated with cellular adhesion, influencing the fate of ProSGs during *in vitro* culture.

Analysis of transcriptomic changes caused by *CDH18* deficiency through RNA-seq

To investigate the regulatory mechanism of CDH18 in ProSG

growth, ProSGs were collected at 72 h post-CDH18 or scrambled siRNA transfection for transcriptome sequencing. Principal component analysis (PCA) indicated high consistency within the same groups and evident differences between the two groups (Figure 3A), confirming the reliability and consistency of the datasets. Analysis identified a total of 722 DEGs, including 630 up-regulated and 92 down-regulated DEGs, based on a threshold of $|Log_2(\text{fold-change})|>0.5$) (Supplementary Table S3), as shown in the volcano plot in Figure 3B.

To further explore the role of CDH18 in ProSG fate, the 722 DEGs were subjected to GO and KEGG pathway enrichment analyses (Supplementary Tables S4, S5). GO analysis highlighted enrichment in various biological processes, including positive regulation of cell proliferation, growth factor activity, cell adhesion, basement membrane, and positive regulation of cell migration (Figure 3C). KEGG analysis revealed enrichment in various pathways, including PI3K-AKT signaling pathway, tight junctions, Rap1 signaling pathway, cell adhesion molecules (CAMs), TGF-β signaling pathway, MAPK signaling pathway, and Wnt signaling pathway (Figure 3D). Notably, the enriched GO terms and KEGG pathways were predominantly involved in cell adhesion processes and signaling pathways. These observations are consistent with our cellular level findings, suggesting that *CDH18* down-regulation influences the expression of other cell adhesion genes. Subsequent analysis of genes associated with cell adhesion, focal adhesion, and cell adhesion molecules showed that the expression levels of *CLDN1*, *CLDN6*, *CLDN9*, *CLDN11*, *ITGA1*, *ITGA3*, *ITGA8*, *ITGA11*, *CDH2*, *JAM2*, and *JAM3* were significantly elevated in ProSGs transfected with CDH18 siRNA compared to the control group (Figure 3E–G). To validate the transcriptomic data, several adhesion-related DEGs (e.g., *CLDN9*, *CLDN11*, *ADGRG1*, *JAM2*, and *ITGA1*) were randomly selected for RT-PCR validation. Results confirmed the up-regulation of most genes, such as *JAM2*, *CDH2*, *CLDN11*, *CLDN9*, and *COL15A1*, consistent with the transcriptomic findings (Figure 3H). We also focused on the PI3K-AKT and Wnt signaling pathways, which are pivotal for spermatogonia proliferation (Takase & Nusse, 2016; Wu et al., 2008). Although KEGG analysis indicated that the two signaling pathways were affected by *CDH18* knockdown, GSEA showed no marked changes in the expression of these pathways (data not shown). Examining the expression of genes involved in the PI3K-AKT and Wnt signaling pathways revealed that neither *PI3K* nor *AKT* was activated (Figure 3I). Both the cell proliferation-associated gene *CCND1* and the inhibitor gene *CDKN1A* were up-regulated (Figure 3I). Furthermore, both Wnt signaling pathway activators (*FZD1*, *FZD10*, *SFRP2*, *SFRP4*, *DAAM2*, and *WNT5A)* and inhibitors (*DKK2* and *NKD2*) were up-regulated (Figure 3J). According to our experimental protocols, ProSGs were transfected with siRNA on day 2 of culture, followed by a medium change on day 3, and harvested after an additional 72 h. At this point, the cells had been cultured *in vitro* for 6 days. Cell growth in the control group already showed a decline, while the CDH18 siRNA-treated group maintained a good growth condition (Figure 2C–F). Therefore, the DEGs associated with the PI3K and Wnt signaling pathways likely reflect a decline in expression levels in the control group rather than an increase in the CDH18 siRNA-treated group. This suggests that although *CDH18* disruption affects the expression of some genes in the PI3K-AKT and Wnt signaling pathways, these pathways were not effectively activated. In summary, *CDH18* knockdown in ProSGs enhanced the expression of genes associated with cell adhesion, adherence, and growth. However, the underlying mechanism remains unclear and may involve compensatory effects, where the expression of many adhesion-related genes is activated to compensate for the loss of CDH18 function. Interestingly, a similar phenomenon was observed in our previous study where knockout of *Cdh1* in mouse SSCs promoted the expression of *Cdh22* (Song et al., 2022), indicating that this compensatory mechanism may not be unique to ProSGs.

Impact of *Cdh18* deficiency using knockout mice

To elucidate the role of CDH18 in germ cell development and the underlying biological mechanisms, *Cdh18*-deficient mice were generated utilizing CRISPR-Cas9-mediated gene editing to delete the third exon of the *Cdh18* gene (Figure 4A). The resulting genotype was validated at both the genomic (Figure 4B) and protein levels (Figure 4C). Morphological, size, and histological analyses of neonatal and adult testes from homozygous $Cdh18^{-/-}$ and wild-type $Cdh18^{+/+}$ mice demonstrated no significant differences (Supplementary Figure S2A–D), suggesting that *Cdh18* loss does not impair testicular development. However, a slight increase in PLZF-positive cells was observed in the testes of $Cdh18^{-/-}$ mice relative to their $Cdh18^{+/+}$ counterparts, although this increase was not statistically significant (Figure 4D, E). Sperm motility assays showed reduced activity in $Cdh18^{-/-}$ mice, although this decrease did not reach statistical significance (Figure 4F). Fertility assessments conducted through crossbreeding experiments involving $Cdh18^{-/-}$ and $Cdh18^{+/-}$ mice yielded litter sizes ranging from 4.0 to 6.25, with no significant deviation from the progeny counts of control C57BL/6L mice (Figure 4G). These findings suggest that *Cdh18* deficiency does not markedly impair testicular development or male fertility.

To further investigate the impact of *Cdh18* loss on testicular function, we focused on the expression of genes integral to spermatogonia differentiation, including *c-kit*, *Stra8*, *Sohlh2*, and *Sycp3*. No discernible alterations in expression levels were detected compared to the wild-type controls. However, an up-regulation in *Axin2* mRNA was noted (Figure 4H), consistent with our prior research demonstrating the role of CDH1 in the maintenance of SSCs niche adherence in murine models through β-catenin binding (Song et al., 2022). Our earlier studies also established that porcine CDH22 contains a catenin-binding domain and interacts with PI3K, β-catenin, and JAK2 in female germline stem cells (FGSCs) (Zhang et al., 2018, 2019). Building on these findings, we explored the potential interactions between murine CDH18 and the Wnt, JAK-STAT, PTEN, and PI3K-AKT signaling pathways. Purified SSCs from wild-type mice expressing both CDH18 and CDH1 (Figure 4I) were harvested for co-immunoprecipitation assays, which revealed associations between CDH18 and β-catenin, JAK2, and PTEN, but not PI3K (Figure 4J), suggesting that CDH18 integrates into the Wnt, JAK-STAT, and PTEN signaling networks. Western blot analyses were employed to further examine expression changes in pivotal genes related to these signaling pathways and SSC self-renewal. Results showed down-regulation of PTEN, RAD51, PDK1, AKT3, GSK-3β, AXIN2, β-catenin, and Cyclin D1 in the absence of CDH18, alongside diminished phosphorylation of AKT3 and β-catenin, indicating that neither the PI3K-AKT nor Wnt signaling

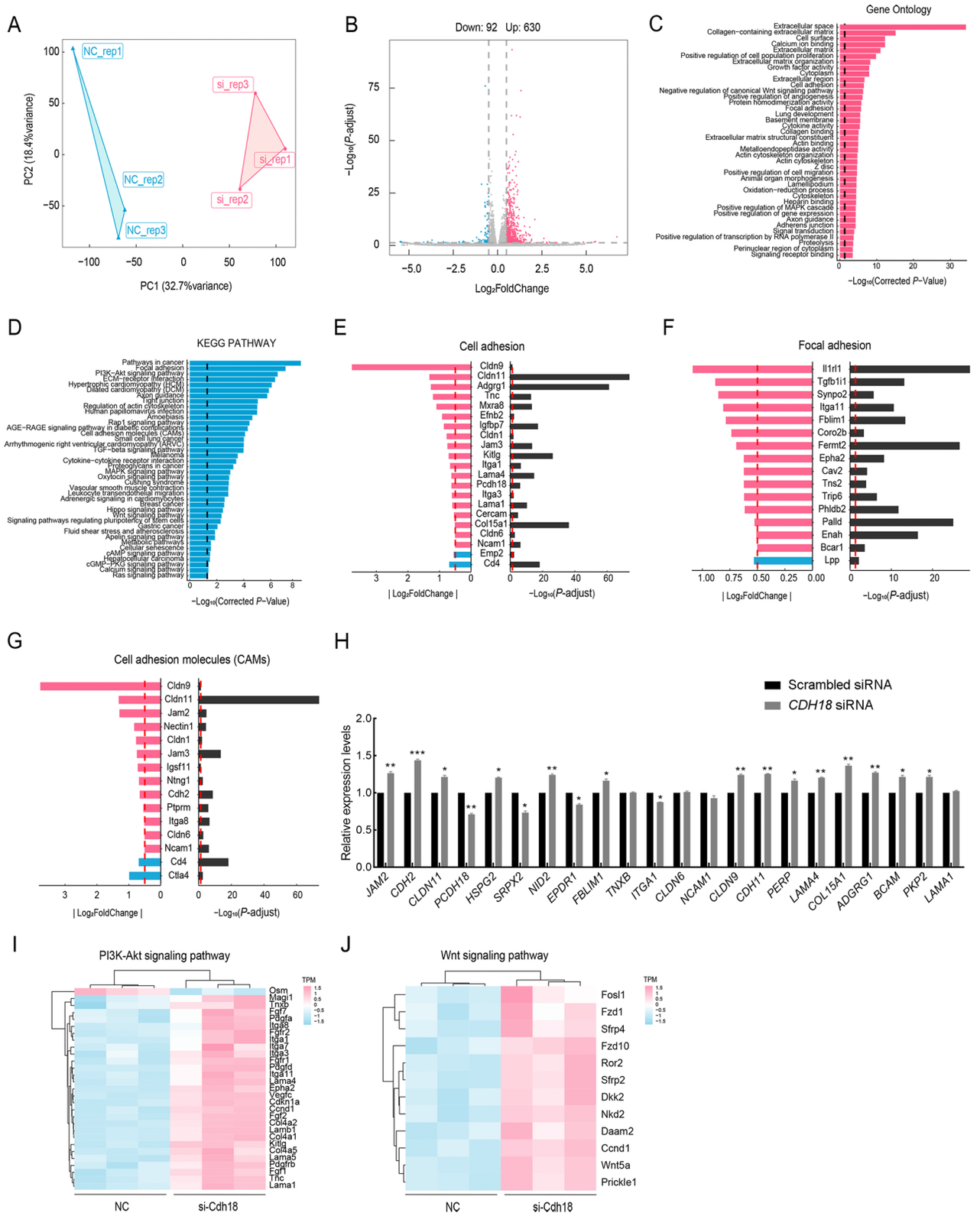

Figure 3 Analysis of transcriptomic changes caused by *CDH18* disturbance

A: PCA analysis of samples from testes of ProSGs transfected with CDH18 siRNA or scrambled siRNA. B: Volcano plot of DEGs. C: GO terms enriched in DEGs. D: KEGG pathways enriched in DEGs. E–G: Expression changes in genes related to cell adhesion, focal adhesion, and cell adhesion molecules. H: Randomly selected DEGs related to adhesion were validated using RT-PCR. I, J: Expression changes in genes related to PI3K-AKT and Wnt signaling pathways. Data are mean±SD, *: P<0.05; **: P<0.01; ***: P<0.001; ns: Not significant.

pathways were activated (Figure 4K). Moreover, the expression of the SSC marker PLZF was not markedly altered, suggesting that SSC numbers were unaffected. Previous studies have demonstrated that reduced phosphorylation levels at sites S675 and S33/S37/T41 of β-catenin, due to decreased expression of β-catenin, lead to

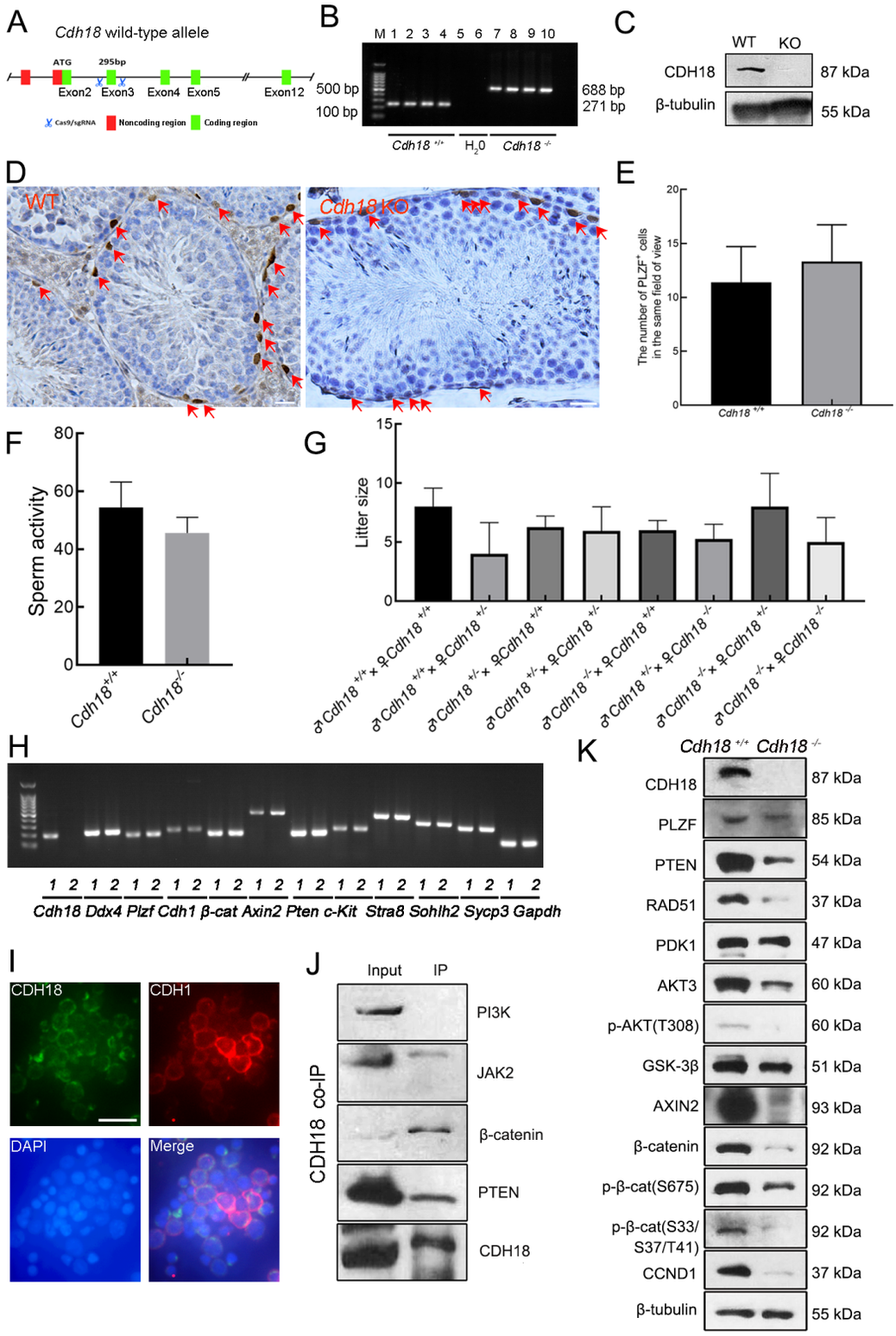

Figure 4 Construction of *Cdh18* knockout mice and characterization of phenotypes

A: Schematic of exon 3 knockout in mouse *Cdh18* driven by CRISP-Cas9. B: Genotype of progeny mice detected using PCR. C: Expression of CDH18 protein from wild-type and *Cdh18* knockout mice detected using western blotting. D: Immunohistochemical analysis showing PLZF staining in testes from 60-day-old $Cdh18^{+/+}$ and $Cdh18^{-/-}$ mice. Scale bar: 20 μm. E: Number of $PLZF^{+}$ cells in 200× view from $Cdh18^{+/+}$ and $Cdh18^{-/-}$ testes. F: Sperm activity from $Cdh18^{+/+}$ and $Cdh18^{-/-}$ mice. G: Average litter sizes in $Cdh18^{+/+}$×$Cdh18^{-/-}$, $Cdh18^{+/-}$×$Cdh18^{-/-}$, $Cdh18^{+/+}$×$Cdh18^{+/-}$, and $Cdh18^{+/+}$×$Cdh18^{-/-}$, $Cdh18^{+/-}$×$Cdh18^{+/-}$, and $Cdh18^{-/-}$×$Cdh18^{-/-}$ crossings. H: Expression levels of *Cdh18*, *Ddx4*, *Plzf*, *Cdh1*, *β-catenin*, *Axin2*, *Pten*, *c-kit*, *Stra8*, *Sohlh2*, *Sycp3*, and *Gapdh* in $Cdh18^{+/+}$ and $Cdh18^{-/-}$ SSCs detected using RT-PCR. I: Expression levels of CDH18 and CDH1 in purified wild-type SSCs detected using immunofluorescence. Scale bar: 20 μm. J: Co-IP assay showing interaction between CDH18 and PI3K, JAK2, β-catenin, and PTEN. K: Expression levels of CDH18, PTEN RAD51, PDK1, AKT3, p-AKT(T308), GSK3-β, AXIN2, β-catenin, p-β-catenin (S675), p-β-catenin (S33/S37/T41), Cyclin D1, and β-tubulin in the testes of $Cdh18^{+/+}$ and $Cdh18^{-/-}$ detected using western blot analysis.

reduced SSC self-renewal and proliferation. Therefore, we hypothesize that the absence of *CDH18* enhances cell adhesion, potentially reducing detachment from the feeder layer and subsequent cell death, thereby extending the duration of *in vitro* culture. Given the down-regulation of pivotal genes for proliferation and self-renewal, we propose that *Cdh18*-deficient SSCs are more likely to enter a "quiescent state".

Gene expression profiles of *Cdh18* deficiency through transcriptomic analysis

To assess the impact of *Cdh18* deficiency on gene expression profiles, we performed transcriptomic analysis of testes harvested from both *Cdh18*$^{-/-}$ and *Cdh18*$^{+/-}$ mice. The PCA results demonstrated high consistency within each group and significant differences between the groups (Figure 5A). A total of 1 086 DEGs were up-regulated and 883 DEGs were down-regulated, based on a threshold of $|\text{Log}_2(\text{fold-change})|>0.5$, as illustrated in the volcano plot and heatmap in Figure 5B, C.

GO analysis revealed significant enrichment in genes involved in cell adhesion and extracellular molecule binding, including "regulation of cell-cell adhesion", "regulation of cell junction assembly", "regulation of cell-substrate adhesion", "G protein-coupled receptor binding", "laminin binding", and "extracellular matrix binding" (Figure 5D). Furthermore, KEGG

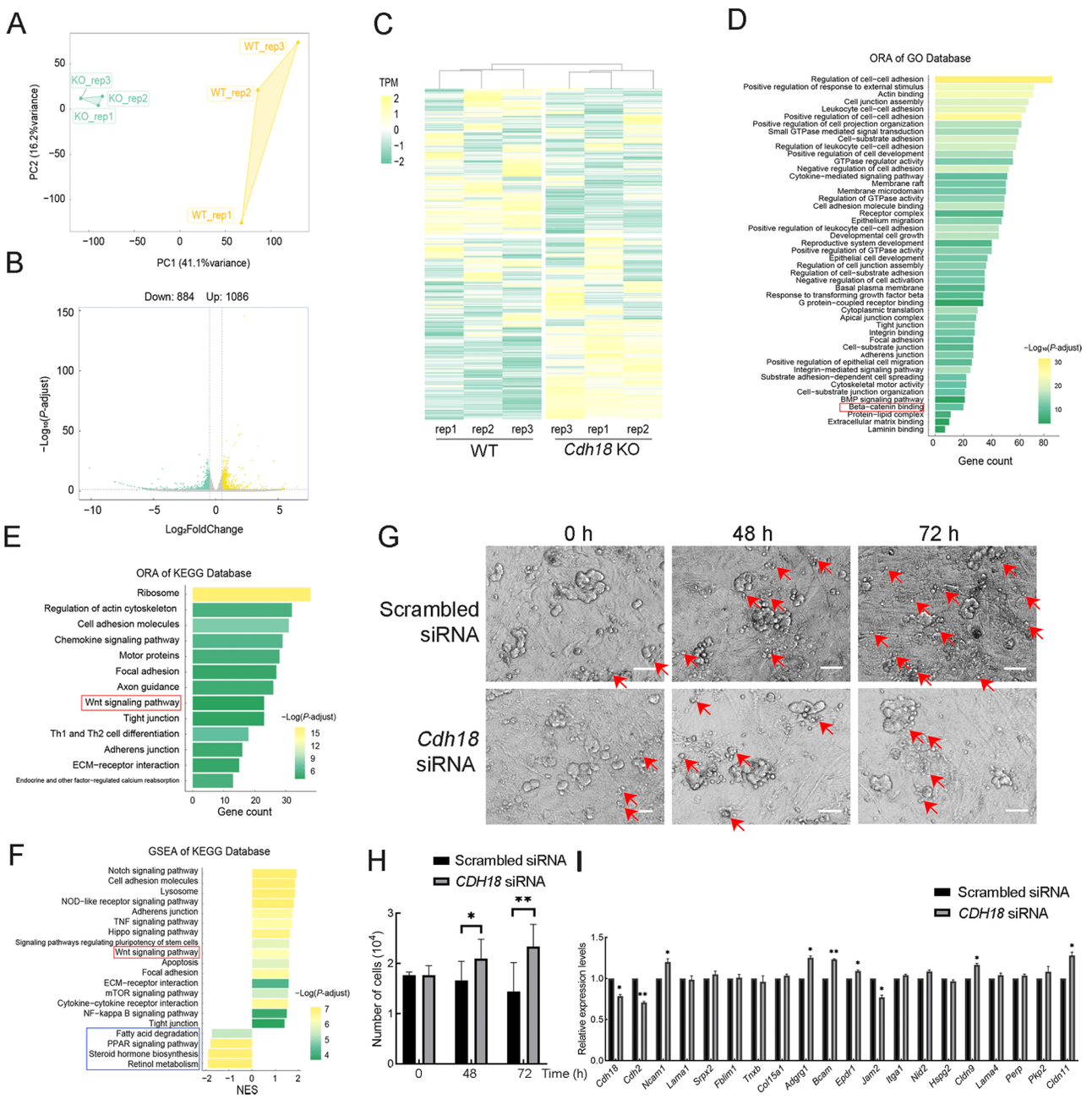

Figure 5 Comparison of transcriptomic patterns in testes from *Cdh18*$^{-/-}$ and *Cdh18*$^{+/-}$ mice

A: PCA of samples from testes of *Cdh18*$^{-/-}$ and *Cdh18*$^{+/-}$ mice. B, C: Volcano plot and heatmap of DEGs in *Cdh18*$^{-/-}$ and *Cdh18*$^{+/-}$ mouse testes. D, E: GO terms and KEGG pathways enriched in DEGs. F: Correlation of enriched DEGs in KEGG pathways with *Cdh18* deficiency analyzed using GSEA. G: SSCs cultured *in vitro* for 48 h were transfected with scrambled or Cdh18 siRNA, then incubated for 72 h (red arrows indicate dead SSCs). H: SSC numbers at 0 h, 48 h, and 72 h post-transfection. I: After 72 h of incubation with siRNA, SSCs were harvested to detect expression of adhesion-associated genes using RT-PCR. Data are mean±SD, *: $P<0.05$; **: $P<0.01$. Scale bar: 20 μm.

pathway analysis revealed enrichment in “cell adhesion molecules”, “chemokine signaling pathway”, “adherens junction”, “ECM-receptor interaction”, “focal adhesion”, and “tight junction” (Figure 5E). To further validate the changes in adhesion-related genes, we analyzed variations in genes within the categories related to cell adhesion, including “regulation of cell-cell adhesion”, “positive regulation of cell-cell adhesion”, and “cell-substrate adhesion”, and observed that many genes were up-regulated (Supplementary Figure S3A–C). The GSEA results also demonstrated a significant increase in the “cell adhesion molecules” cluster (Supplementary Figure S3D), consistent with our other findings. Furthermore, these results closely mirror those observed in porcine ProSGs following *CDH18* disruption, thus validating the phenotypic and genotypic similarities and affirming the suitability of this transgenic mouse model for studying the corresponding mechanisms in porcines. Notably, the “β-catenin binding” and “Wnt signaling pathway” were enriched in the GO and KEGG analyses, respectively, suggesting β-catenin as a potential key factor driving the observed phenotypic alterations.

Further analysis of the GSEA results revealed an up-regulation in “cell adhesion molecules”, “cytokine-cytokine receptor interaction”, “adherens junction”, “focal adhesion”, “ECM-receptor interaction”, and “tight junction” (Figure 5F), indicating enhanced cell adhesion following *Cdh18* loss, consistent with the observations in porcine ProSGs. Conversely, pathways crucial for spermatogonial differentiation and cell proliferation, such as “retinol metabolism” and “PPAR signaling”, were down-regulated. Within the PPAR signaling pathway, enriched genes, including *Cyp4a12b*, *Ilk*, *Cyp4a32*, *Cyp4a10*, *Fabp1*, *Cyp4a14*, *Cyp4a12a*, *Apoa1*, *Apoc3*, and *Apoa5*, primarily associated with fatty acid metabolism, were similar to those in the “fatty acid degradation” category. These findings suggest an inhibition of retinoic acid and fatty acid metabolism in *Cdh18*-deficient SSCs. Importantly, the Notch, Hippo, TNF, Wnt, and mTOR signaling pathways were activated in the *Cdh18* knockout mice, suggesting potential involvement in regulating cell adhesion and metabolism post-*Cdh18* deficiency in SSCs. To verify these results, mouse SSCs cultured on MEF feeder for 48 h were transfected with scrambled or Cdh18-siRNA for 72 h. Results showed no significant differences in SSC growth status between the control and *Cdh18* knockdown groups at 48 h post-transfection. However, at 72 h post-transfection, the control group exhibited deteriorated cell growth, with a decrease in colony number and an increase in dead cells. In contrast, the knockdown group maintained a stable growth status, with no remarkable change compared to the 48 h mark (Figure 5G). The average passage time for mouse SSCs is 5 days. On day 5, SSC growth status in the control group deteriorated, while cells in the knockdown group maintained a relatively stable state without a significant increase in number. Cell counting revealed that SSCs with *Cdh18* knockdown were stably maintained after 5 days of *in vitro* culture, whereas the control group experienced a significant decrease in cell number due to poor health (Figure 5H). Subsequently, RT-PCR assays were conducted to examine the expression of cell adhesion-related genes. Results indicated that following *Cdh18* knockdown, the expression levels of multiple adhesion-related genes (e.g., *Ncam1*, *Adgrg1*, *Bcam*, *Epdr1*, *Cldn9*, and *Cldn11*) significantly increased (Figure 5I). These findings are consistent with those observed in knockdown experiments conducted on porcine ProSGs.

Previous studies have shown that β-catenin promotes proliferation and self-renewal in SSCs (Song et al., 2022; Takase & Nusse, 2016) and is involved in metabolic processes, such as activating mTORC1 to stimulate cell growth via energy metabolism. Thus, we concluded that the down-regulation of *β-catenin* caused by *Cdh18* knockout may be a critical event driving SSCs into a quiescent state.

Mechanism of enhanced ProSGs adhesion following *CDH18* down-regulation

To clarify the mechanism of CDH18-β-catenin interaction in porcine ProSGs, we compared the sequences of CDH18 preproproteins from humans (NP_001336488.1) and porcines (XP_020932622.1) and found a high sequence identity of 98% (Figure 6A). As the human CDH18 protein contains a β-catenin binding domain (Shibata et al., 1997), we hypothesized that porcine CDH18 may similarly bind to β-catenin and show an association with the Wnt signaling pathway. Co-IP assays confirmed the binding of CDH18 and β-catenin in porcine ProSGs (Figure 6B). Furthermore, a remarkable decrease in β-catenin expression due to CDH18 disturbance was observed (Figure 6C, D), implying that the down-regulation of β-catenin is associated with CDH18 loss. Thus, we propose that decreased CDH18 expression in ProSGs affects β-catenin expression, thereby influencing cell fate.

Intrigued by the potential involvement of CDH18 in the PI3K-AKT and JAK-STAT signaling pathways, similar to CDH22, we conducted further Co-IP assays. These experiments demonstrated the association of CDH18 with JAK2 and PI3K in ProSGs, substantiating its role in modulating these pathways. Correspondingly, CDH18 deficiency resulted in decreased expression of *JAK2*, *STAT3*, and *PIK3CG* in ProSGs (Figure 6C, D), indicating JAK-STAT and PI3K-AKT signaling pathway inactivation due to *CDH18* loss, consistent with the transcriptomic results indicating the suppression of genes involved in these pathways. Given the pivotal roles of the JAK-STAT, PI3K-AKT, and Wnt signaling pathways in SSC self-renewal and proliferation (Takase & Nusse, 2016; Wu et al., 2008), our data suggest that the absence of CDH18 impairs critical signaling mechanisms essential for these processes. This impairment potentially triggers activation of adhesion-related genes as a compensatory mechanism, potentially culminating in cellular quiescence. The proposed regulatory schema is depicted in Figure 6E. Nonetheless, further investigation is required to elucidate the precise mechanisms underlying these interactions, especially the connection between the down-regulation of CDH18 and activation of multiple adhesion-associated genes.

DISCUSSION

The homing and transition of ProSGs into SSCs are fundamental processes for spermatogenesis. SSCs possess remarkable self-renewal and differentiation capabilities, leading to the continuous production of spermatozoa throughout life. These cells serve as exemplary models for breeding, clinical therapies, and gene therapies due to their unique properties. However, the paucity of progenitor spermatogonia within mammalian testes presents a significant challenge in harvesting adequate numbers for research and application. In this study, we explored the regulatory patterns

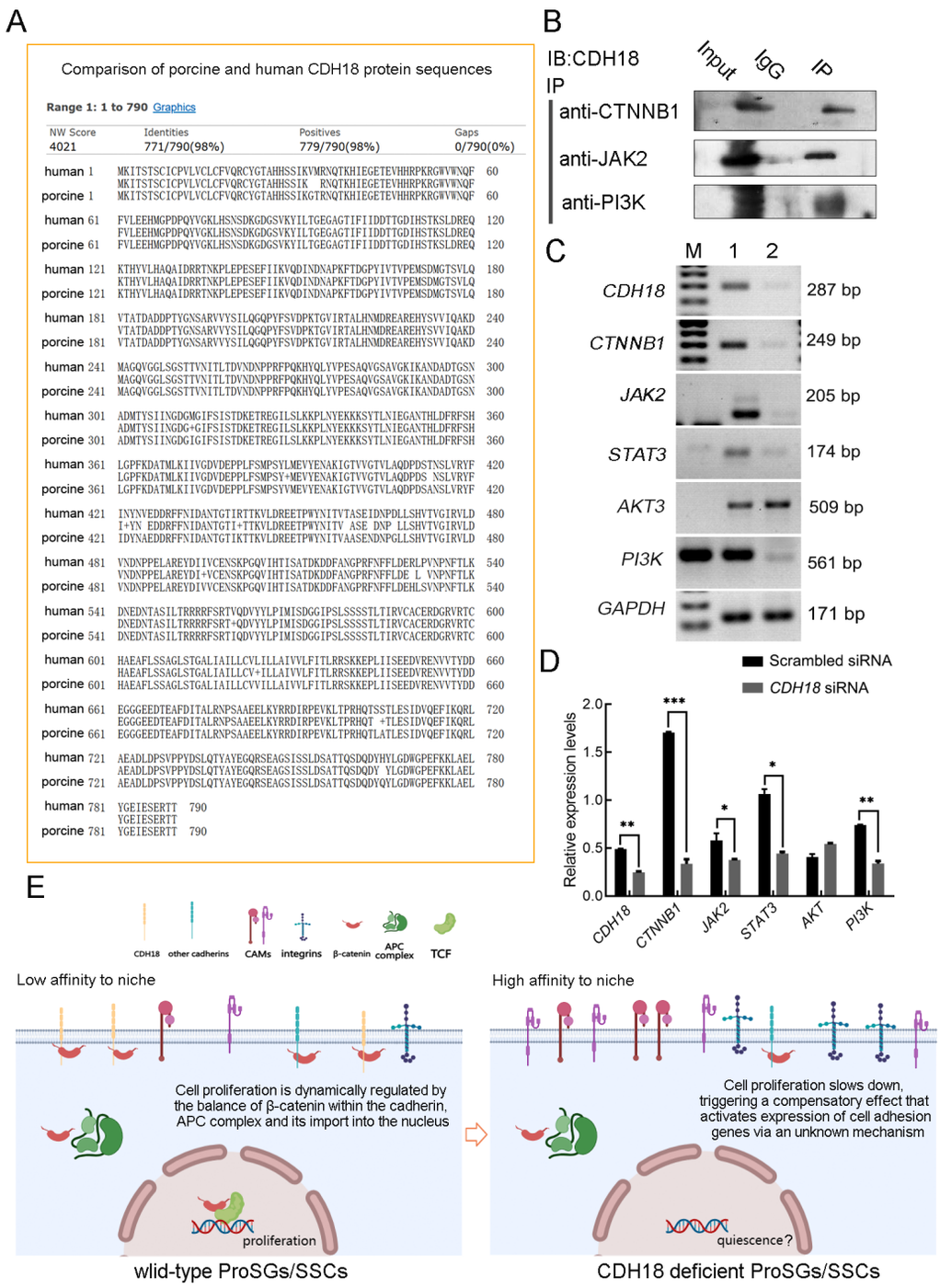

Figure 6 Analysis of interactions between CDH18 and β-catenin, JAK2, and PI3K

A: Porcine and human CDH18 protein sequences were compared. B: Binding of CDH18 to β-catenin, JAK2, and PI3K detected using Co-IP. C: Expression levels of *CDH18*, *β-catenin*, *JAK2*, *STAT3*, *PIK3CG*, and *AKT1* in ProSGs transfected with scrambled or CDH18 siRNA detected using RT-PCR. D: Relative expression levels of *CDH18*, *β-catenin*, *JAK2*, *STAT3*, *PIK3CG*, and *AKT1* in ProSGs transfected with scrambled or CDH18 siRNA detected using RT-PCR normalized to *GAPDH*. E: Regulatory effects of CDH18 on ProSG/SSC proliferation and quiescence. Data are mean±SD, *: P<0.05; **: P<0.01; ***: P<0.001.

of pivotal membrane molecules on ProSG/SSC functions. Notably, we discovered that *Cdh18* knockout in mouse testes did not affect the histological morphology of the testes, number of PLZF^{+} cells, sperm motility, or ability to produce offspring. Consequently, we determined that *Cdh18* knockout does not impact the homing and transition of ProSGs into SSCs, nor does it affect subsequent spermatogenesis. Interestingly, CDH18 loss impacted several key signaling pathways associated with cell proliferation, as identified by transcriptomic analysis (Figure 3D). Examination of DEGs involved in the PI3K-AKT and Wnt signaling pathways—two pivotal pathways for SSC proliferation—revealed that these pathways were not efficiently activated. Western blot results further confirmed this conclusion, showing down-regulated expression of AKT, β-catenin, and Cyclin D1. We also observed several discrepancies between mRNA and protein

detection results. For instance, *CyclinD1*, *Plzf*, and *Axin2* were up-regulated at the mRNA level but down-regulated at the protein level. These inconsistencies may be attributed to post-transcriptional regulation or feedback regulatory mechanisms of the proteins. However, further experiments are required to validate this hypothesis and fully understand the underlying mechanisms.

Our initial exploration into the *in vitro* culture of porcine ProSGs demonstrated that isolated ProSGs began forming small colonies within 2–3 days. As the culture progressed, the number of colonies increased, and distinct cellular boundaries became apparent. Subculturing was necessary by days 5 or 6 to maintain cell viability, as overly large colonies adversely affected cell survival. Upon *CDH18* expression interference, early observations indicated no significant changes in cell count, proliferation rate, or colony size compared to the control group. However, as the culture period extended, considerable differences emerged. By day six, a subset of control cells began to detach from the feeder layer due to a lack of passaging, whereas the ProSGs in the *CDH18* knockdown group exhibited no such detachment. This trend intensified by day 8, with a significant number of floating control cells observed, while the *CDH18* knockdown group remained stable. Based on these findings, we hypothesize that *CDH18* interference may influence cell adhesion properties.

Consistent with GO and KEGG pathway analyses, adhesion-related processes and pathways were notably enriched. Validation through RT-PCR confirmed the transcriptomic results, showing increased expression of several adhesion-related genes (including *CLDN9*, *CLDN11*, *ADGRG1*, *JAM2*, *ITGA1*, *CDH2*, and *COL15A1*), thereby substantiating the impact of *CDH18* interference on cell adhesion. Interestingly, the loss of *CDH18* in both porcine and murine models resulted in a marked up-regulation of genes associated with cell adhesion. This suggests that cadherin loss in SSCs may trigger a compensatory effect. Similarly, in our previous study, *Cdh1* deficiency in murine SSCs led to the up-regulation of *Cdh22*, which rescued *β-catenin* expression and mitigated differentiation (Song et al., 2022). The mechanisms underlying this compensatory effect remain largely enigmatic, particularly given its apparent independence of the Wnt and JAK-STAT signaling pathways, despite CDH18 interacting with β-catenin and JAK2. The activation of AKT following *CDH18* deficiency, alongside the down-regulation of PI3K, hints at the involvement of alternative pathways, including those mediated by G-protein-coupled receptors or integrins. Although up-regulation of genes related to GTPase activity, GTP binding, and integrin binding was noted, further experimentation is necessary to validate these findings.

In summary, this study elucidated the biological function of CDH18 in porcine ProSGs and mouse spermatogonia, emphasizing its potential role in regulating cell interactions and quiescence. CDH18 is intricately linked with multiple signaling pathways, including PI3K-AKT, JAK-STAT, and Wnt, through direct interactions. Our investigation into the role of CDH18 within porcine ProSGs provides valuable insights for refining *in vitro* culture systems and advancing our understanding of ProSG fate determination. Despite these findings, molecular foundations of these relationships are not yet fully understood. Future studies should delineate the interaction patterns of CDH18 with other extracellular molecules to deepen our comprehension of SSC biology and enhance *in vitro* culture methodologies.

DATA AVAILABILITY

RNA sequencing data were deposited in the NCBI (PRJNA1045800), China National Center for Bioinformation (PRJCA025330), and Science Data Bank databases (DOI: 10.57760/sciencedb.18158).

SUPPLEMENTARY DATA

Supplementary data to this article can be found online.

COMPETING INTERESTS

The authors declare that they have no competing interests.

AUTHORS' CONTRIBUTIONS

X.X.L. carried out the isolation and culture of porcine ProSGs and performed molecular and cellular experiments. D.C.Z. managed the *Cdh18* knockout (KO) mice and delineated their phenotypes. Y.W. contributed to the collection of data on *Cdh18* KO mice and performed transcriptomic analyses. J.W. conducted bioinformatics analyses. X.J.W., R.J., J.R.L., Y.N.L., and H.H.L. were involved in handling the mouse models. Y.L.C. contributed to cell isolation and immunostaining. W.H.X. analyzed the data and secured financial support. P.H. contributed to study design and data analysis. Z.F.X. conceived the study and acquired funding support. K.Z. was the principal investigator who conceived and designed the study, coordinated the research activities, secured funding, and drafted the manuscript. All authors read and approved the final version of the manuscript.

REFERENCES

Aponte PM, Soda T, Teerds KJ, et al. 2008. Propagation of bovine spermatogonial stem cells in vitro. *Reproduction*, **136**(5): 543–557.

Brigidi GS, Bamji SX. 2011. Cadherin-catenin adhesion complexes at the synapse. *Current Opinion in Neurobiology*, **21**(2): 208–214.

Brinster RL. 2002. Germline stem cell transplantation and transgenesis. *Science*, **296**(5576): 2174–2176.

Brinster RL, Zimmermann JW. 1994. Spermatogenesis following male germ-cell transplantation. *Proceedings of the National Academy of Sciences of the United States of America*, **91**(24): 11298–11302.

Caires K, Broady J, Mclean D. 2010. Maintaining the male germline: regulation of spermatogonial stem cells. *Journal of Endocrinology*, **205**(2): 133–145.

Chen X, Long F, Cai B, et al. 2017. A novel relationship for schizophrenia, bipolar and major depressive disorder Part 5: a hint from chromosome 5 high density association screen. *American Journal of Translational Research*, **9**(5): 2473–2491.

Clermont Y, Perey B. 1957. Quantitative study of the cell population of the seminiferous tubules in immature rats. *American Journal of Anatomy*, **100**(2): 241–267.

Dadoune JP. 2007. New insights into male gametogenesis: what about the spermatogonial stem cell niche?. *Folia Histochemica et Cytobiologica*, **45**(3): 141–147.

De Rooij DG, Russell LD. 2000. All you wanted to know about spermatogonia but were afraid to ask. *Journal of Andrology*, **21**(6): 776–798.

Espeseth A, Johnson E, Kintner C. 1995. *Xenopus F-cadherin*, a novel member of the cadherin family of cell adhesion molecules, is expressed at boundaries in the neural tube. *Molecular and Cellular Neuroscience*, **6**(3): 199–211.

Foty RA, Steinberg MS. 2005. The differential adhesion hypothesis: a direct evaluation. *Developmental Biology*, **278**(1): 255–263.

Fujihara M, Kim SM, Minami N, et al. 2011. Characterization and *in vitro* culture of male germ cells from developing bovine testis. *Journal of Reproduction and Development*, **57**(3): 355–364.

Gallardo T, Shirley L, John GB, et al. 2007. Generation of a germ cell-

specific mouse transgenic Cre line. *Vasa-Cre. Genesis*, **45**(6): 413–417.
Goel S, Sugimoto M, Minami N, et al. 2007. Identification, isolation, and in vitro culture of porcine gonocytes. *Biology of Reproduction*, **77**(1): 127–137.
Halbleib JM, Nelson WJ. 2006. Cadherins in development: cell adhesion, sorting, and tissue morphogenesis. *Genes & Development*, **20**(23): 3199–3214.
Hirano S, Takeichi M. 2012. Cadherins in brain morphogenesis and wiring. *Physiological Reviews*, **92**(2): 597–634.
Hogan C, Serpente N, Cogram P, et al. 2004. Rap1 regulates the formation of E-cadherin-based cell-cell contacts. *Molecular and Cellular Biology*, **24**(15): 6690–6700.
Johnson E, Theisen CS, Johnson KR, et al. 2004. R-cadherin influences cell motility via Rho family GTPases. *Journal of Biological Chemistry*, **279**(30): 31041–31049.
Junghof J, Kogure Y, Yu T, et al. 2022. CDH18 is a fetal epicardial biomarker regulating differentiation towards vascular smooth muscle cells. *npj Regenerative Medicine*, **7**(1): 14.
Kanatsu-Shinohara M, Miki H, Inoue K, et al. 2005. Germline niche transplantation restores fertility in infertile mice. *Human Reproduction*, **20**(9): 2376–2382.
Kimura Y, Matsunami H, Inoue T, et al. 1995. Cadherin-11 expressed in association with mesenchymal morphogenesis in the head, somite, and limb bud of early mouse embryos. *Developmental Biology*, **169**(1): 347–358.
Kubota H, Brinster RL. 2006. Technology insight: *in vitro* culture of spermatogonial stem cells and their potential therapeutic uses. *Nature Clinical Practice Endocrinology & Metabolism*, **2**(2): 99–108.
Lee KH, Lee WY, Kim JH, et al. 2016. Subculture of germ cell-derived colonies with GATA4-positive feeder cells from neonatal pig testes. *Stem Cells International*, **2016**: 6029271.
Lee WY, Park HJ, Lee R, et al. 2013. Establishment and *in vitro* culture of porcine spermatogonial germ cells in low temperature culture conditions. *Stem Cell Research*, **11**(3): 1234–1249.
Luo JP, Megee S, Rathi R, et al. 2006. Protein gene product 9.5 is a spermatogonia-specific marker in the pig testis: application to enrichment and culture of porcine spermatogonia. *Molecular Reproduction and Development*, **73**(12): 1531–1540.
Luo JK, Treubert-Zimmermann U, Redies C. 2004. Cadherins guide migrating Purkinje cells to specific parasagittal domains during cerebellar development. *Molecular and Cellular Neuroscience*, **25**(1): 138–152.
Maeda M, Johnson KR, Wheelock MJ. 2005. Cadherin switching: essential for behavioral but not morphological changes during an epithelium-to-mesenchyme transition. *Journal of Cell Science*, **118**(Pt 5): 873–887.
McGuinness MP, Orth JM. 1992. Reinitiation of gonocyte mitosis and movement of gonocytes to the basement membrane in testes of newborn rats in vivo and in vitro. *The Anatomical Record*, **233**(4): 527–537.
Nakagawa S, Takeichi M. 1995. Neural crest cell-cell adhesion controlled by sequential and subpopulationspecific expression of novel cadherins. *Development*, **121**(5): 1321–1332.
Niedenberger BA, Geyer CB. 2018. Advanced immunostaining approaches to study early male germ cell development. *Stem Cell Research*, **27**: 162–168.
Orwig KE, Ryu BY, Avarbock MR, et al. 2002. Male germ-line stem cell potential is predicted by morphology of cells in neonatal rat testes. *Proceedings of the National Academy of Sciences of the United States of America*, **99**(18): 11706–11711.
Redies C. 2000. Cadherins in the central nervous system. *Progress in Neurobiology*, **61**(6): 611–648.
Reintsch WE, Habring-Mueller A, Wang RW, et al. 2005. β-Catenin controls cell sorting at the notochord-somite boundary independently of cadherin-mediated adhesion. *The Journal of Cell Biology*, **170**(4): 675–686.
Sahare M, Kim SM, Otomo A, et al. 2016. Factors supporting long-term culture of bovine male germ cells. *Reproduction, Fertility and Development*, **28**(12): 2039–2050.
Shibata T, Shimoyama Y, Gotoh M, et al. 1997. Identification of human cadherin-14, a novel neurally specific type II cadherin, by protein interaction cloning. *Journal of Biological Chemistry*, **272**(8): 5236–5240.
Song WX, Zhang DC, Mi JQ, et al. 2022. E-cadherin maintains the undifferentiated state of mouse spermatogonial progenitor cells via β-catenin. *Cell & Bioscience*, **12**(1): 141.
Sun YZ, Liu ST, Li XM, et al. 2019. Progress in *in vitro* culture and gene editing of porcine spermatogonial stem cells. *Zoological Research*, **40**(5): 343–348.
Suzuki S, Sano K, Tanihara H. 1991. Diversity of the cadherin family: evidence for eight new cadherins in nervous tissue. *Cell Regulation*, **2**(4): 261–270.
Takase HM, Nusse R. 2016. Paracrine Wnt/β-catenin signaling mediates proliferation of undifferentiated spermatogonia in the adult mouse testis. *Proceedings of the National Academy of Sciences of the United States of America*, **113**(11): E1489–E1497.
Tanihara H, Kido M, Obata S, et al. 1994a. Characterization of cadherin-4 and cadherin-5 reveals new aspects of cadherins. *Journal of Cell Science*, **107**(Pt 6): 1697–1704.
Tanihara H, Sano K, Heimark RL, et al. 1994b. Cloning of five human cadherins clarifies characteristic features of cadherin extracellular domain and provides further evidence for two structurally different types of cadherin. *Cell Adhesion and Communication*, **2**(1): 15–26.
Wang JJ, Li JM, Xu W, et al. 2019. Androgen promotes differentiation of $PLZF^+$ spermatogonia pool via indirect regulatory pattern. *Cell Communication and Signaling*, **17**(1): 57.
Wang JJ, Tian HR, Liu HY, et al. 2023. Low dose of zearalenone inhibited the proliferation of porcine prospermatogonia and transformed the physiology through cytokine-cytokine receptor interaction. *Theriogenology*, **211**: 49–55.
Wu J, Zhang Y, Tian GG, et al. 2008. Short-type PB-cadherin promotes self-renewal of spermatogonial stem cells via multiple signaling pathways. *Cellular Signalling*, **20**(6): 1052–1060.
Yamada M, De Chiara L, Seandel M. 2016. Spermatogonial stem cells: implications for genetic disorders and prevention. *Stem Cells and Development*, **25**(20): 1483–1494.
Zhang DC, Chen R, Cai YH, et al. 2020. Hyperactive reactive oxygen species impair function of porcine Sertoli cells via suppression of surface protein ITGB1 and connexin-43. *Zoological Research*, **41**(2): 203–207.
Zhang PF, Chen XX, Zheng Y, et al. 2017. Long-term propagation of porcine undifferentiated spermatogonia. *Stem and Development*, **26**(15): 1121–1131.
Zhang XY, Wei R, Sun YZ, et al. 2019. AKT3 Is a pivotal molecule of cadherin-22 and GDNF family receptor-α1 signal pathways regulating self-renewal in female germline stem cells. *Stem Cells*, **37**(8): 1095–1107.
Zhang XY, Yang Y, Xia Q, et al. 2018. Cadherin 22 participates in the self-renewal of mouse female germ line stem cells via interaction with JAK2 and β-catenin. *Cellular and Molecular Life Sciences*, **75**(7): 1241–1253.
Zheng Y, Tian XE, Zhang YQ, et al. 2013. In vitro propagation of male germline stem cells from piglets. *Journal of Assisted Reproduction and Genetics*, **30**(7): 945–952.
Zou K, Wang J, Bi HW, et al. 2019. Comparison of different in vitro differentiation conditions for murine female germline stem cells. *Cell Proliferation*, **52**(1): e12530.